Stable isotope homogenization of polar firn and ice

S. J. Johnsen

Abstract. $\delta(^{18}O)$-cycles with wavelengths shorter than 20 cm of ice are obliterated during firnification. This corresponds to a diffusion length of 7–8 cm of ice, independent of accumulation rate and temperature, according to a model presented. Another combined ice flow-diffusion model describes the observed smoothing of $\delta(^{18}O)$-gradients at great depths. Based on digital deconvolution techniques, a method is described that allows re-establishing apparently lost $\delta(^{18}O)$-cycles. This may considerably extend the range of ice core dating by annual $\delta(^{18}O)$-cycles.

L'homogénéisation du névé et de la glace polaire par l'utilisation des isotopes stables

Résumé. Les cycles de $\delta(^{18}O)$ avec des longueurs d'onde inférieures à 20 cm de glace sont effacés durant la transformation du névé. Ceci correspond à une longueur de diffusion de 7–8 cm de glace, indépendante du taux d'accumulation et de la température selon le modèle présenté. Un autre modèle, combinant écoulement de la glace et diffusion, décrit l'amortissement des gradients de $\delta(^{18}O)$ observé à grandes profondeurs. On décrit une méthode basée sur des techniques de déconvolution qui permet de ré-établir les cycles de $\delta(^{18}O)$ apparemment perdus. Ceci peut étendre de façon considérable les possibilités de datation des carottes de glace à partir des cycles annuels de $\delta(^{18}O)$.

DIFFUSION IN SNOW AND FIRN

Detailed $\delta(^{18}O)$-profiles through the upper firn layers of polar ice caps show that the gradients are being gradually smoothed with depth down to at least 15–20 m. This effect, first mentioned by Langway (1967), is demonstrated in Fig. 1(A) showing a continuous $\delta(^{18}O)$-profile based on 1-cm samples from the surface down to a depth of 11.35 m at station Milcent (central Greenland). The firnification process is evidently associated with strong vertical mixing.

It is generally accepted that densification in the upper firn layers takes place by rearrangement of the grains resulting in closer packing. Assuming that the grains are rearranged by passing the vapour phase (some of the grains are growing and changing their shape, while others are unstable and disappear) the diffusion of the water molecule in the pore space would seem to be responsible for the vertical mixing observed.

Barometric pumping may also contribute, but hardly to any appreciable extent, since frequent impermeable ice and crust layers in the Dye 3 core (south Greenland) has not prevented considerable smoothing of the $\delta(^{18}O)$-profile (Dansgaard *et al.*, 1973, p. 24). Temperature gradients could to some extent contribute to the mixing, but, since such gradients are present only close to the surface, their overall contribution is probably not important.

Further investigation of the processes involved leads to the following assumptions about the firnification process:

(1) The rate of densification is only dependent on the density and the mean vapour pressure in the firn.

(2) The vertical rate of mixing is a function of the same parameters and, furthermore, of the diffusion constant of water vapour in air.

(3) The mixing essentially ceases when the critical density $\rho_c = 0.55$ g/cm^3 is reached, corresponding to the closest random packing of grains.

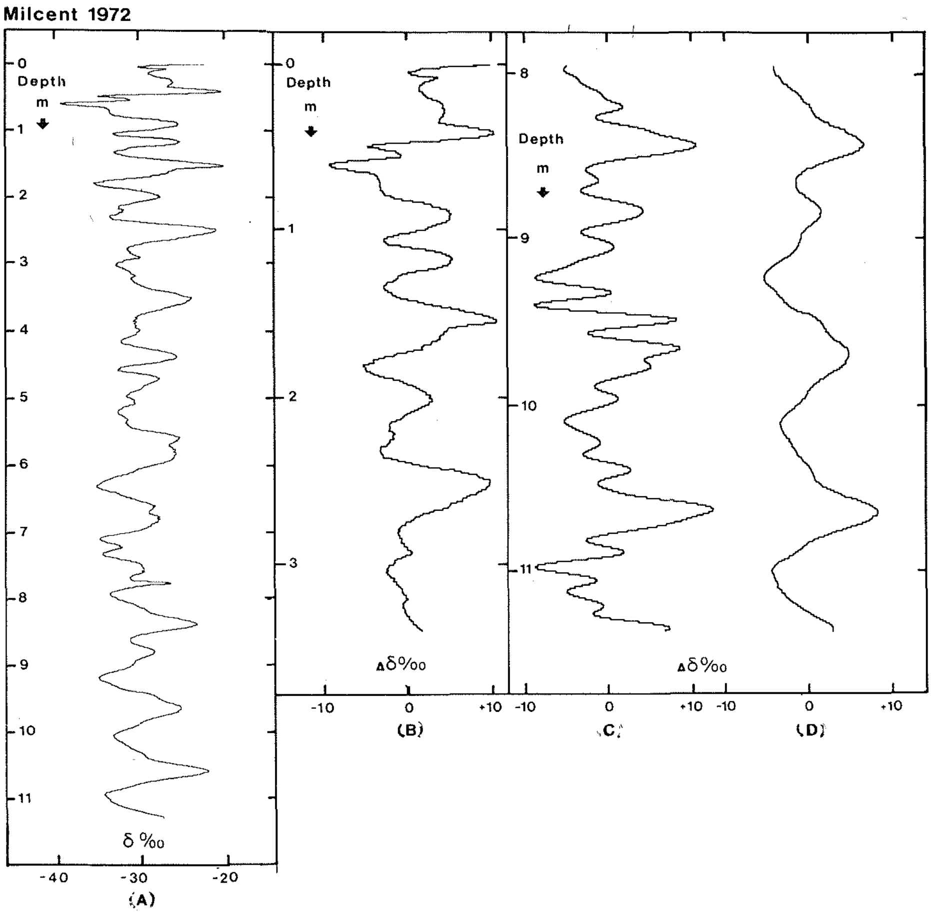

FIGURE 1. A detailed δ(^{18}O)-profile based on continuous 1-cm samples. (A) is the entire profile, (B) and (D) the upper and lower part of it respectively. (C) is the lower pa deconvoluted, $L = 8$ cm, $\epsilon = 0.2^0/_{00}$.

Assumption (1) may be written

$$\frac{dv_p}{dt} = -c_1 p v_p; \qquad v_p = \frac{1}{\rho} - \frac{1}{\rho_i} \tag{1}$$

v_p being the volume of pore space per kilogramme of snow, t the time since the deposition; p the vapour pressure; c_1 a constant; and ρ and ρ_i the densities of firn and ice, respectively.

According to the Benson (1962) densification model,

$$\frac{dv_p}{d\sigma} = -mv_p; \qquad \sigma = At \tag{2}$$

σ being the load; A the accumulation rate [kg m^{-2} year^{-1}]; and m a constant depending on local conditions.

Combining (1) and (2) gives

$$mA = c_1 p \tag{3}$$

Values of m derived from measured density profiles have been published (Benson, 1962). Usually, A is also known. One way of checking the validity of equation (3) is to make an Arrhenius plot of mA as a function of the reciprocal temperature for various profiles. If equation (3) is valid the apparent activation energy Q should equal that of water vapour (12.2 kcal mol^{-1}). Figure 2 shows such a plot. All known Greenland density profiles and most Antarctic ones are in good agreement with the model showing that c_1 is generally independent of the location, perhaps with the exception of areas of extremely low accumulation and temperature, due to the relatively heavy load on layers of low density.

In the following, some important consequences of the model will be shown by simplified calculations.

The fraction of the firn in the vapour phase is $r = c_2 p v_p$, c_2 being a constant. During the residence time τ_v of the water molecule in the pore space, its vertical

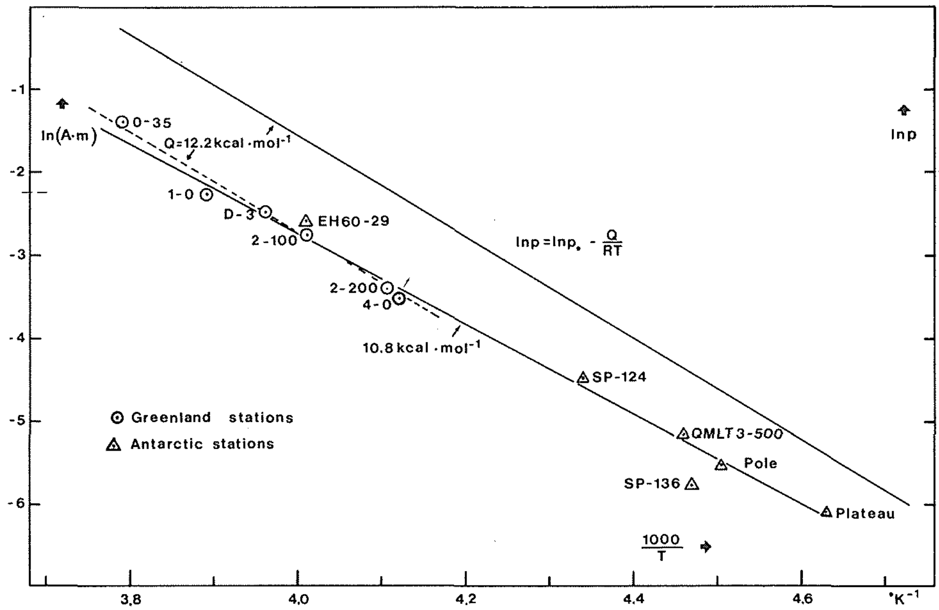

FIGURE 2. Logarithmic plot of Am (year^{-1}), to the left, and p (mm Hg), to the right, *versus* T^{-1}.

mean square displacement is

$$\Delta L_f^2 = 2D\tau_v\left(\frac{2}{\pi}\right)^2$$

D being the diffusion constant of the water molecule in air.

The residence time τ_s in the solid phase is of the order of τ_v/r, and the rate of change of L_f^2 therefore of the order of

$$\frac{dL_f^2}{dt} \simeq \frac{\Delta L_f^2}{\tau_s} \simeq Dr = Dc_2 p v_p$$

which, according to (1), is

$$\frac{dL_f^2}{dt} = -D\frac{c_2}{c_1}\frac{dv_p}{dt} \rightarrow \frac{dL_f^2}{dv_p} = -\frac{c_2}{c_1}D$$

or

$$L_f^2 = \frac{c_2}{c_1}D(v_{p0} - v_p) \tag{4}$$

Due to the necessary approximations involved, this formula cannot be expected to be quantitatively correct. However, it does show the important point that the diffusion length is independent of the accumulation rate and only slightly dependent (through D) on the temperature. It is worth noting that in the derivation of equation (4) no assumption was made about p being constant, which should account for temperature gradients in the firn.

The smoothing effect of the diffusive mass transport in the firn may be described by the well-known formula for the ratio R between the final and the initial amplitude of a $\delta(^{18}O)$-cycle of wavelength A cm of ice:

$$R = \exp\left(-2\pi^2 L_f^2 / A^2\right) \tag{5}$$

With slight modifications this formula is valid for all of the isotopic components of water. L_f determines the lower limit of A, for which a $\delta(^{18}O)$-cycle is still detectable after the firnification ($R = 0.05$).

The value of L_f may be estimated from the experiences with ice cores from locations of widely different glaciological regimes. For example, in Greenland the annual $\delta(^{18}O)$-cycles are obliterated at North Site with $A = 17$ cm, but not at Crête with $A = 27$ cm (Dansgaard *et al.*, 1973), [*cf.* Fig. 7(c)], nor at Summit with $A = 25$ cm (Hammer, 1977); and at Vostok, Antarctica, with $A = 2.7$ cm (Barkov, 1975), the shortest $\delta(^{18}O)$-oscillations found below 138 m depth have a wavelength of 25 cm (Dansgaard *et al.*, 1977). Consequently, the above-mentioned lower value of A is close to 20 cm of ice, corresponding to $L_f = 7$–8 cm of ice for $R = 0.05$, according to equation (5) (*cf.* Fig. 3). This means that after the firnification the water molecules are, on the average, displaced 7–8 cm of ice from their initial positions in the core (disregarding the sinking of the layers and their thinning by vertical strain).

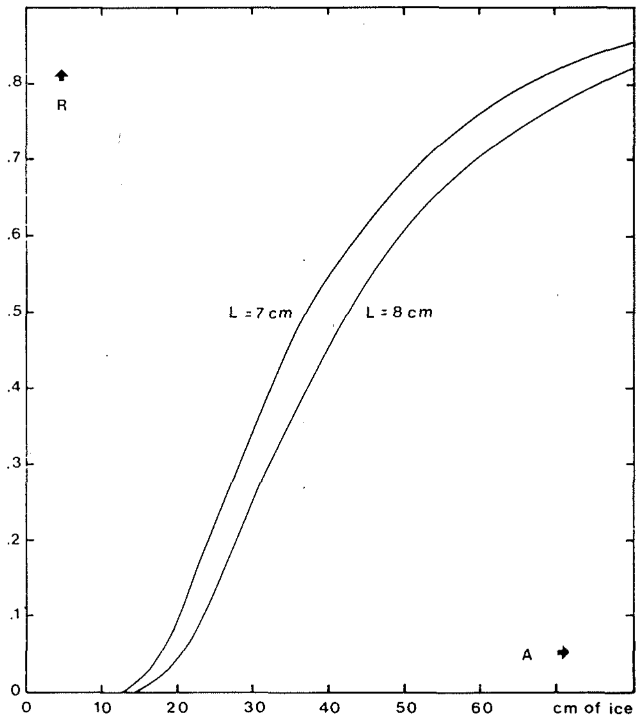

FIGURE 3. The relative amplitude of a harmonic $\delta(^{18}O)$-cycle of A cm wavelength for diffusion lengths of 7 and 8 cm respectively.

DIFFUSION IN SOLID ICE

After firnification, further smoothing takes place only by diffusion in solid ice. Following a layer as it sinks, and assuming that its vertical strain rate $\dot{\varepsilon}_z$ and its self-diffusion constant D_i (determined by the *in situ* temperature) are known as functions of time t, we can write the diffusion equation for the layer as

$$\frac{\partial \delta}{\partial t} = D_i(t)\frac{\partial^2 \delta}{\partial z^2} - \dot{\varepsilon}_z(t) z \frac{\partial \delta}{\partial z} \tag{6}$$

Note that z is the vertical axis of a coordinate system, the origin of which is fixed within the layer considered, and that the layer is being uniformly strained within that coordinate system.

This equation can be solved for the initial condition $\delta(^{18}O) = \delta(z; 0)$ for $t = 0$:

$$\delta(z; t) = \frac{1}{L(t)\sqrt{(2\pi)}}\int_{-\infty}^{+\infty} \delta\left(z' \exp\left(-\int_0^t \dot{\varepsilon}_z(\tau)\mathrm{d}\tau\right); 0\right)\exp\left(-\tfrac{1}{2}(z - z')^2/L^2(t)\right)\mathrm{d}z' \tag{7}$$

$L(t)$ being the solution to the differential equation

$$\frac{1}{2}\frac{\mathrm{d}L^2}{\mathrm{d}t} - \dot{\varepsilon}_z(t)L^2 = D(t): \tag{8}$$

$$L^2(t) = \exp\left(2\int_0^t \dot{\varepsilon}_z(\tau)\,\mathrm{d}\tau\right)\left[2\int_0^t D(\tau)\exp\left(-2\int_0^\tau \dot{\varepsilon}_z(\theta)\,\mathrm{d}\theta\right)\mathrm{d}\tau + L_f^2\right] \tag{9}$$

where L_f is the diffusion length at time 0, i.e. at the firn-ice boundary. Using $L_f = 7$–8 cm we include the diffusion during firnification in the calculations.

The ratio R for a $\delta(^{18}O)$-cycle of initial wavelength A cm of ice is calculated as

$$R = \exp(-2\pi^2 L^2/A^{*2}) \tag{10}$$

where

$$A^* = A\exp\left(\int_0^t \dot{\varepsilon}_z(\tau)\,\mathrm{d}\tau\right) \tag{11}$$

In fact A^* is the thickness of an annual layer t years after deposition.

The solutions to equations (7)–(11) have to be based on an ice dynamic model, which, for each particle trajectory, gives the vertical strain rate, annual layer thickness, and temperature as a function of time.

Such calculations have been performed by flow models similar to those of Dansgaard and Johnsen (1969) and Philbert and Federer (1971). The models have been generalized to work along arbitrary flow lines, and they take into account (a) Glen's law, (b) the upstream accumulation rate, (c) ice thickness, (d) bedrock topography, (e) divergence of ice flow, and (f) surface temperature. The temperature field in the ice is calculated on a two-dimensional grid, consistent with the flow vectors and the frictional heating within the ice. The flow vectors and the temperature distribution in the ice are recalculated until stable solutions are found.

The diffusion constant is adopted from Ramseier (1967):

$D_i = D_{i0}\exp(-Q/RT)$, where $D_{i0} = 12.5\ \mathrm{cm^2\,s^{-1}}$, and $Q = 14.4\ \mathrm{kcal\,mol^{-1}}$.

Since D_i is highly dependent on temperature, the results are quite sensitive to the actual temperature profiles generated by the models. One way of improving the calculations would be to adopt non-stationary temperature profiles as generated by the glacial to interglacial temperature shifts, in which case the heat conduction equation has to be integrated deep into bedrock. Examples of such improved models will be presented in a coming publication.

Figures 4–6 present calculated profiles of age, annual layer thickness and *R*-values for Camp Century, Milcent and Crête, all in Greenland. The calculated steady-state δ(^{18}O)-profile for Milcent is also included in Fig. 5.

Detailed δ(^{18}O)-measurements on increments of the Camp Century deep core have been published by Johnsen *et al.* (1972), showing annual δ(^{18}O)-cycles at

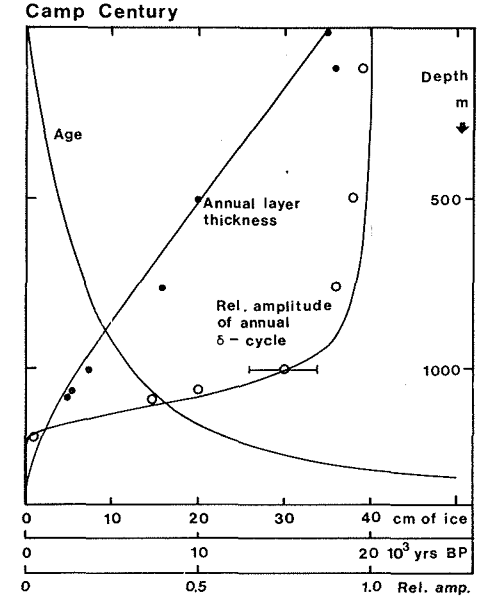

FIGURE 4. Flow model/ice diffusion calculations with data from the Camp Century deep ice core.

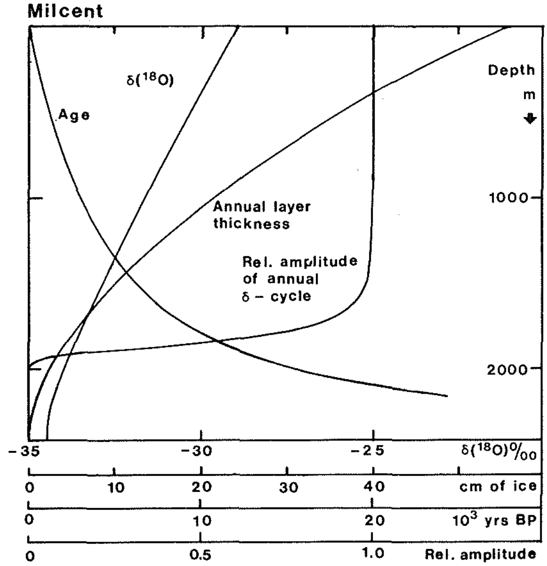

FIGURE 5. Flow model/ice diffusion calculations for Milcent, including steady-state δ(^{18}O)-profile.

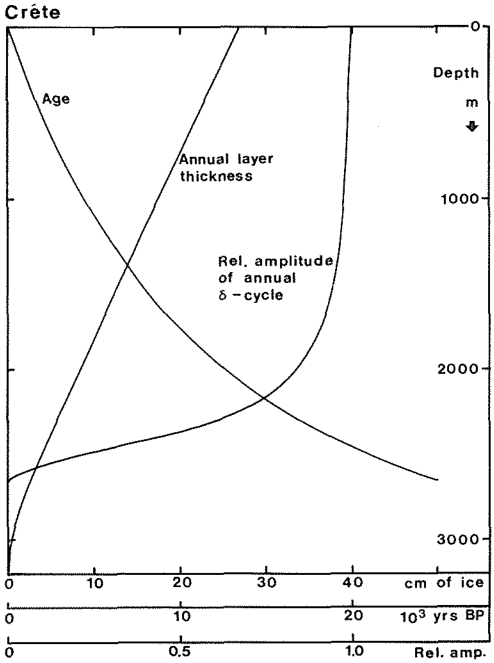

FIGURE 6. Flow model/ice diffusion calculations for Crête; note long lifetime of annual $\delta(^{18}O)$-cycles.

various depths. The corresponding annual layer thicknesses and the R-values deduced from this data have been plotted in Fig. 4. The agreement with the model calculations is seen to be quite satisfactory.

The calculation for station Crête indicates that the annual $\delta(^{18}O)$-cycles may survive diffusion for almost 20 000 years compared to approximately 10 000 years at the two other stations. This is due to favourable conditions at Crête (medium accumulation and low temperature as well as great ice thickness). This long lifetime of annual $\delta(^{18}O)$-cycles is one of the reasons why Crête has been selected a potential deep drilling site under the Greenland Ice Sheet Program (GISP).

DECONVOLUTION ('REVERSED DIFFUSION')

In this section it will be shown how it is possible by a 'reversed diffusion' technique to re-establish the initial shape of a $\delta(^{18}O)$-profile smoothed by diffusion. The technique allows a considerable extension of the range of ice core dating by annual $\delta(^{18}O)$-cycles.

As demonstrated by equation (7), the effect of diffusion on a $\delta(^{18}O)$-profile $\delta_0(z)$ is mathematically equivalent to convolving the profile with a symmetrical filter

$$F_1 = \exp[-\tfrac{1}{2}(z - z')^2/L^2]/L\sqrt{(2\pi)}$$

The transfer function (frequency response) of F_1 is

$$\bar{F}_1(k, L) = \exp(-\tfrac{1}{2}k^2L^2) \qquad (12)$$

$k = 2\pi/A$ being the wavenumber and $\bar{F}_1$ the Fourier transform of F_1.

The practical importance of equation (12) is that it allows the design of deconvolution filters which, applied on a smoothed $\delta(^{18}O)$-profile δ_a, rebuild the original one (δ_0) to various degrees of fidelity depending on the sampling length and the noise (due to analyses, sampling and handling) in the measured record, δ_m.

The transfer function of such a filter F has of course to be the inverse of F_1, i.e. $\bar{F} = \bar{F}_1^{-1}$, except for the higher frequencies where strong damping has to be introduced in order to avoid blowing up the noise in the record. Modification of the filter F without loosing too much information is accomplished by employing the technique of optimum filter design.

We now write the measured profiles as a sequence of numbers $\delta_{mi} = \delta_{ai} + \varepsilon_i$, ε_i being white noise, normally of standard deviation 0.1–0.2$^0/_{00}$ depending on the quality of the data, and δ_{ai} the 'signal' we are looking for.

The transfer function of the optimum filter for extracting the signal δ_{ai} is (Wiener, 1949)

$$\bar{F}_2 = \frac{|\bar{\delta}_a|^2}{|\bar{\delta}_a|^2 + |\bar{\varepsilon}|^2}$$

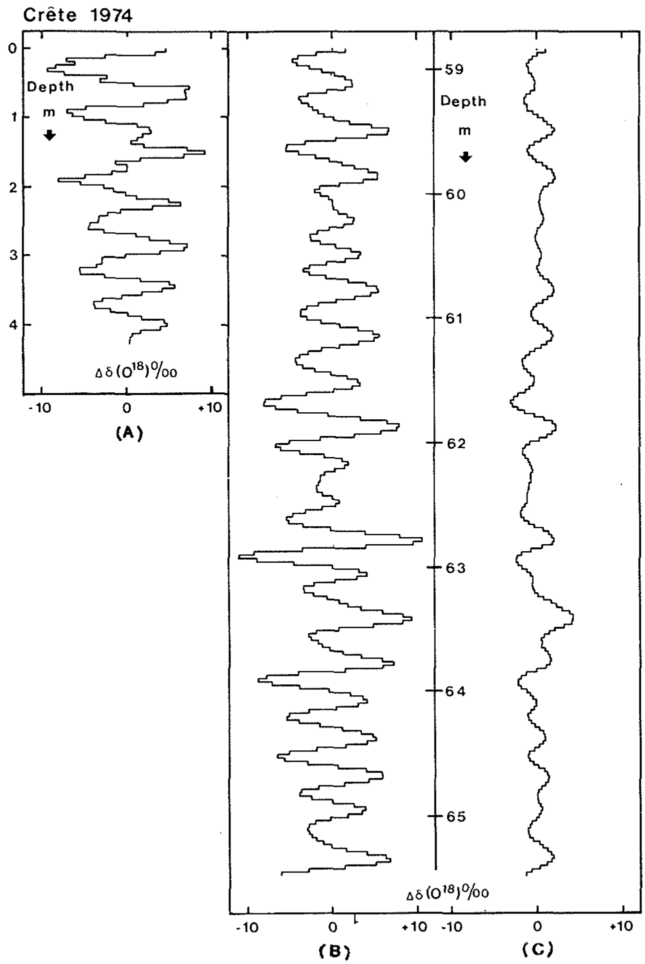

FIGURE 7. (A) an unsmoothed surface $\delta(^{18}O)$-profile, (C) a $\delta(^{18}O)$-profile smoothed by diffusion in firn, (B) the same profile deconvoluted by $L = 8$ cm and $\epsilon = 0.1^0/_{00}$.

Furthermore, the smoothing induced by using samples of finite length Δz instead of spot samples may be corrected for by applying the inverse of the transfer function

$$\bar{F}_3 = \sin(k\,\Delta z/2)/(k\,\Delta z/2)$$

Having specified the properties of the individual filters the overall transfer function to be used on the δ_m series is

$$\bar{F} = \bar{F}_2/(\bar{F}_1 \cdot \bar{F}_3)$$

Once $\bar{F}$ is determined, a symmetric filter F having the specified transfer characteristics can be calculated by the method described by Hibler (1972).

This technique has been applied on various δ_m series:

(a) Fig. 1(D) shows the lower part of the δ_m-profile from Milcent. The result of the application of the deconvolution technique is shown in Fig. 1(C) for comparison with the upper part of δ_m-profile shown in Fig. 1(B). The features of the deconvoluted curve closely resembles those in the uppermost metre in Fig. 1(B).

(b) Fig. 7(A) shows annual δ_m-cycles in the upper firn at Crête. Figure 7(C) is a δ_m-series in the depth interval 59–65 m. In Fig. 7(B) it has been deconvoluted into close resemblance with Fig. 7(A).

(c) The smooth δ_m-curve in Fig. 8 is from an increment of the Camp Century ice core, 1156 m below surface, and approximately 12 000 years old. L is only 1.8 cm due to the considerable thinning of the layers. The strongly oscillating curve shows the result of 'reversed diffusion' through 12 000 years. Cycles that were apparently obliterated show up again, revealing an annual layer thickness of 3.7 cm.

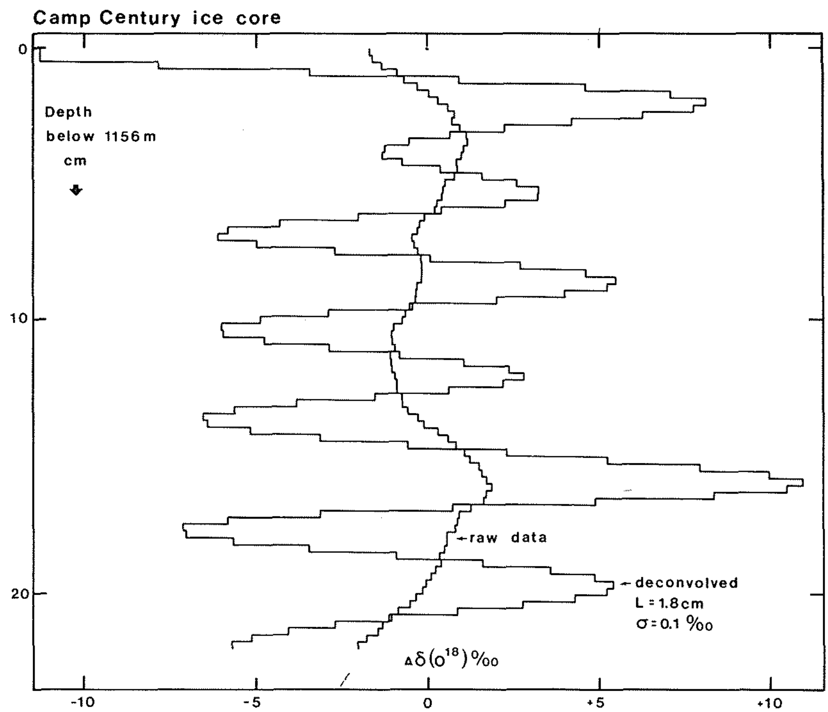

FIGURE 8. δ(^{18}O)-profile from the Camp Century deep ice core smoothed by diffusion in firn and solid ice, measured on approximately 12 000-year-old ice. Deconvolution by $L = 1.8$ cm and $\epsilon = 0.1‰$, establishes the annual layers.

Acknowledgements. The author is indebted to Dr W. Dansgaard for his continuing support, and to Dr W. D. Hibler III for advising on the optimum filter design.

The isotope data were collected under the Greenland Ice Sheet Program, which is supported by the US National Science Foundation, Office of Polar Programs, and the Ministry of Greenland, Copenhagen.

REFERENCES

Barkov, N. I. (1975) Snow accumulation characteristics in the Vostok Station area, 1970 through 1973. *Antarctic J. of the US* **10**, no. 2, 55–56.

Benson, C. (1962) Stratigraphic studies in the snow and firn of the Greenland ice sheet, *US Army Snow, Ice and Permafrost Research Establishment, Research Report no. 70*, 93 pp.

Dansgaard, W. and Johnsen, S. J. (1969) A flow model and a time scale for the ice core from Camp Century, Greenland. *J. Glaciol.* **8**, 215–223.

Dansgaard, W., Johnsen, S. J., Clausen, H. B. and Gundestrup, N. (1973) Stable isotope glaciology. *Medd. Grønland* **197**, no. 2, 5–53.

Dansgaard, W., Barkov, N. I. and Splettstoesser, S. (1977) Stable isotope variations in snow and ice at Vostok, Antarctica. In *Isotopes and Impurities in Snow and Ice* (Proceedings of the Grenoble Symposium, August–September 1975), pp. 204–209: IAHS Publ. no. 118.

Hammer, C. U. (1977) Dating of Greenland ice cores by micro-particle concentration analyses. In *Isotopes and Impurities in Snow and Ice* (Proceedings of the Grenoble Symposium, August–September 1975), pp. 297–301: IAHS Publ. no. 118.

Hibler, W. D. III (1972) Design and maximum error estimation for small error low pass filters. *CRREL Research Report 304.*

Johnsen, S. J., Dansgaard, W., Clausen, H. B. and Langway, C. C. Jr (1972) Oxygen isotope profiles through the Antarctic and Greenland ice sheets. *Nature* **235**, 429–434 and **236**, p. 249.

Langway, C. C. Jr (1967) Stratigraphic analysis of a deep ice core from Greenland. *CRREL Research Report 77.*

Philbert, K. and Federer, B. (1971) On the temperature profile and the age profile in the central part of cold ice sheets. *J. Glaciol.* **10**, no. 58, 3–14.

Ramseier, R. O. (1967) Self-diffusion in ice monocrystals. *CRREL Research Report 232.*

Wiener, N. (1949) *Time series*: The MIT Press, Cambridge, Massachussetts, 1966, 163 pp.

DISCUSSION

Newell:

The profile of $\delta(^{18}O)$ which had been 'restored' showed evidence of biennial oscillation. Has the longer profile also been 'restored' as it would give a long-term record of the occurrence of a biennial oscillation which itself is a parameter of great importance in meteorology?

Dansgaard:

On the face of it, I would be reluctant to draw conclusions about such short periods, because of mass exchange between annual layers by diffusion.

Author's note (added April 1977)

Improved calculation of the diffusion length L to be used in the deconvolution of the δ-profile shown in Fig. 8 gives an L value of 1.2 cm. Using $L = 1.2$ cm in the deconvolution suggests that the number of years in the profile is 10 rather than 6, and that the profile is on the very limit for safe reconstruction of the original annual δ-cycles. The resulting mean annual layer thickness is consequently not greater than 2.2 cm.

Most of the δ-cycles shown in Fig. 8 are most probably blown up biennial oscillations.